JCI The Journal of Clinical Investigation

Inactivation of Notch signaling in the renal collecting duct causes nephrogenic diabetes insipidus in mice

Hyun-Woo Jeong, … , Jin Kim, Young-Yun Kong

J Clin Invest. 2009;119(11):3290-3300. https://doi.org/10.1172/JCI38416.

Research Article **Nephrology**

The heterogeneous cellular composition of the mammalian renal collecting duct enables regulation of fluid, electrolytes, and acid-base homeostasis, but the molecular mechanism of its development has yet to be elucidated. The Notch signaling pathway is involved in cell fate determination and has been implicated in proximal-distal patterning in the mammalian kidney. To investigate the role of Notch signaling in renal collecting duct development, we generated mice in which Mind bomb-1 (Mib1), an E3 ubiquitin ligase required for the initiation of Notch signaling, was specifically inactivated in the ureteric bud of the developing kidney. Mice lacking Mib1 in the renal collecting duct displayed increased urinary production, decreased urinary osmolality, progressive hydronephrosis, sodium wasting, and a severe urinary concentrating defect manifested as nephrogenic diabetes insipidus. Histological analysis revealed a diminished number of principal cells and corresponding increase in the number of intercalated cells. Transgenic overexpression of Notch intracellular domain reversed the altered cellular composition of mutant renal collecting duct, with principal cells occupying the entire region. Our data demonstrate that Notch signaling is required for the development of the mammalian renal collecting duct and principal cell differentiation and indicate that pathway dysregulation may contribute to distal renal tubular disorders.

Find the latest version:

https://jci.me/38416/pdf

Inactivation of Notch signaling in the renal collecting duct causes nephrogenic diabetes insipidus in mice

Hyun-Woo Jeong,[1,2] Un Sil Jeon,[2,3] Bon-Kyoung Koo,[1] Wan-Young Kim,[4] Sun-Kyoung Im,[1,2] Juhee Shin,[1,2] Yunje Cho,[2] Jin Kim,[4] and Young-Yun Kong[1]

[1]Department of Biological Sciences, Seoul National University, Seoul, Republic of Korea. [2]Department of Life Sciences, Pohang University of Science and Technology (POSTECH), Pohang, Kyungbuk, Republic of Korea. [3]Department of Internal Medicine, Korea University Guro Hospital, Seoul, Republic of Korea. [4]Department of Anatomy and MRC for Cell Death Disease Research Center, College of Medicine, Catholic University of Korea, Seoul, Republic of Korea.

The heterogeneous cellular composition of the mammalian renal collecting duct enables regulation of fluid, electrolytes, and acid-base homeostasis, but the molecular mechanism of its development has yet to be elucidated. The Notch signaling pathway is involved in cell fate determination and has been implicated in proximal-distal patterning in the mammalian kidney. To investigate the role of Notch signaling in renal collecting duct development, we generated mice in which Mind bomb-1 (Mib1), an E3 ubiquitin ligase required for the initiation of Notch signaling, was specifically inactivated in the ureteric bud of the developing kidney. Mice lacking Mib1 in the renal collecting duct displayed increased urinary production, decreased urinary osmolality, progressive hydronephrosis, sodium wasting, and a severe urinary concentrating defect manifested as nephrogenic diabetes insipidus. Histological analysis revealed a diminished number of principal cells and corresponding increase in the number of intercalated cells. Transgenic overexpression of Notch intracellular domain reversed the altered cellular composition of mutant renal collecting duct, with principal cells occupying the entire region. Our data demonstrate that Notch signaling is required for the development of the mammalian renal collecting duct and principal cell differentiation and indicate that pathway dysregulation may contribute to distal renal tubular disorders.

Introduction

The early events in mammalian kidney development, such as interactions between the ureteric bud and the metanephric mesenchyme, ureteric bud branching morphogenesis, and induction of glomeruli and nephrons, have been well studied (1–4). However, the development of distal portions of the ureteric bud into a specialized renal collecting duct is poorly understood. The mature renal collecting duct has at least 2 distinct cell types: principal cells and intercalated cells, which are responsible for water and sodium reabsorption and acid-base homeostasis, respectively (5–7). The failure of the ureteric bud to mature into functional collecting ducts has been known to cause renal dysplasia in humans (8). Recently, the forkhead transcription factor Foxi1 has been reported to mediate the differentiation of intercalated cells from epithelial precursor cells and was found to act upstream of intercalated cell–specific proteins such as the solute carrier family 4 (anion exchanger) (AE1) and Pendrin (9). However, the molecular mechanisms of collecting duct development, especially principal cell differentiation, are largely unknown in contrast to the other early events of the kidney development.

The Notch signaling pathway is an evolutionarily conserved intercellular signaling pathway, involved in cell fate determination, differentiation, and tissue-specific gene expression (10). Recent studies have revealed that Notch signaling plays a critical role for the proximal-distal patterning in mammalian kidney development. In vitro mouse kidney organ cultures treated with γ-secretase inhibitor as well as mutant mice missing Presenilin 1 and 2 had reduced numbers of glomerular and proximal tubular epithelial cells (11, 12). Moreover, specific inactivation of Notch2 in the metanephric mesenchyme leads to loss of proximal epithelial cells in the nephron, without affecting the ureteric bud branching morphogenesis or distal tubule development (13). However, previous studies on Notch signaling in kidney development have investigated the development of proximal nephrons, which are derived from metanephric mesenchyme, but not the development of the renal collecting duct, which is derived from ureteric bud, even though Jag1 and Notch2 are expressed in the developing mammalian renal collecting duct (14, 15).

In mammals, Notch signaling is initiated by interactions between the 4 Notch receptors (Notch1–Notch4) and their ligands, Delta-like-1 (Dll-1), Dll3, Dll4, Jagged-1 (Jag1), and Jag2. Recent studies demonstrated that the endocytosis of Notch ligands in the signal-producing cells is absolutely required for the initiation of Notch signaling. Two structurally distinct E3 ubiquitin ligases, Neuralized (Neur) and Mind bomb (Mib), are known to regulate the endocytosis of Notch ligands in Drosophila and zebrafish, respectively (16, 17). In mammals, 2 Neur homologs, Neur1 (18, 19) and Neur2 (20), and 2 Mib homologs, Mind bomb-1 (Mib1) (21) and Mib2 (22), have been identified. Although all 4 E3 ubiquitin ligases are known to induce the endocytosis of Notch ligands in vitro, only Mib1 has an obligatory role in the activation of Jag- as well as Dll-mediated Notch signaling in mammalian development, while Neur1, Neur2, and Mib2 are dispensable (23). Thus, genetic mutation of Mib1 is an excellent model to elucidate the role of Notch signaling in various mammalian tissues (24–28).

Conflict of interest: The authors have declared that no conflict of interest exists.
Citation for this article: *J. Clin. Invest.* **119**:3290–3300 (2009). doi:10.1172/JCI38416.

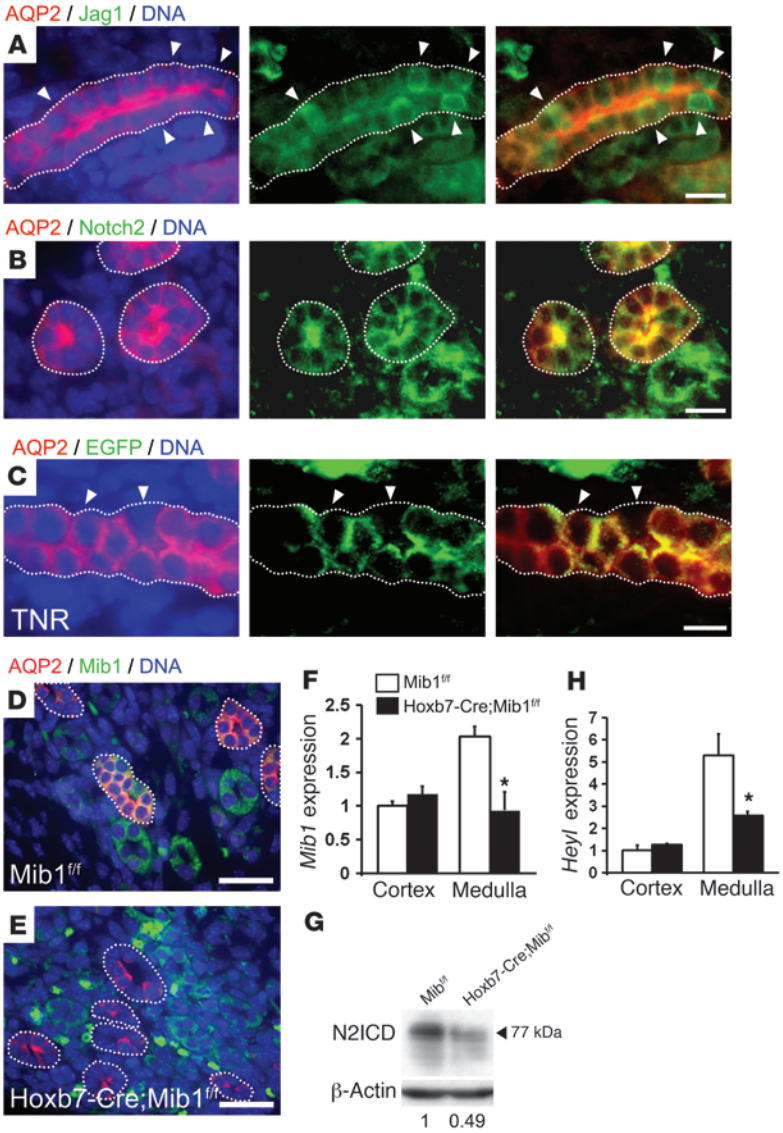

Figure 1
Inactivation of Notch signaling in the collecting duct of *Hoxb7-CreMib1*$^{f/f}$ mouse kidneys. (**A** and **B**) Immunohistochemical staining of E16.5 C57BL/6 mouse embryonic kidneys with anti-Jag1 (**A**, green), anti-Notch2 (**B**, green), and anti-AQP2 (**A** and **B**, red) antibodies. Hoechst (blue) stains DNA, and dotted lines indicate renal collecting ducts. Note the different fluorescent intensities of Jag1 in the collecting duct (**A**, arrowheads). Scale bars: 15 μm. (**C**) Immunohistochemical staining of P0 TNR mouse kidneys with anti-EGFP (green) and anti-AQP2 (red) antibodies. In the collecting ducts, EGFP signals are not detected in AQP2-negative cells (arrowheads). Hoechst (blue) stains DNA, and dotted lines indicate renal collecting ducts. Scale bar: 15 μm. (**D** and **E**) Immunohistochemical staining with anti-Mib1 (green) and anti-AQP2 (red) antibodies in the kidneys of E18.5 *Mib1*$^{f/f}$ (**D**) and *Hoxb7-CreMib1*$^{f/f}$ (**E**) littermates. Hoechst (blue) stains DNA, and dotted lines indicate renal collecting ducts. Scale bars: 30 μm. (**F**) Quantitative real-time RT-PCR analysis of Mib1 in the kidneys of E18.5 *Mib1*$^{f/f}$ and *Hoxb7-CreMib1*$^{f/f}$ littermates. Error bars represent mean ± SD. *$P < 0.05$. (**G**) Western blot analysis of Notch2 intracellular domain (N2ICD) in the kidneys of E18.5 *Mib1*$^{f/f}$ and *Hoxb7-CreMib1*$^{f/f}$ littermates. Numbers indicate relative values of intensity normalized to β-actin. The arrowhead indicates the 77-kDa protein. (**H**) Quantitative real-time RT-PCR analysis of HeyL in the kidneys of E18.5 *Mib1*$^{f/f}$ and *Hoxb7-CreMib1*$^{f/f}$ littermates. Error bars represent mean ± SD. *$P < 0.05$.

To examine the role of Notch signaling in mammalian renal collecting duct development, we specifically inactivated the *Mib1* gene in the renal collecting duct, by crossing Mib1 floxed mice (*Mib1*$^{f/f}$) (23) with Hoxb7-Cre mice that express the Cre recombinase exclusively in the ureteric bud of the developing kidney (29). In these mice (*Hoxb7-CreMib1*$^{f/f}$ mice), Notch signaling was efficiently inactivated in the renal collecting duct. After birth, the *Hoxb7-CreMib1*$^{f/f}$ mice suffered from nephrogenic diabetes insipidus, which is characterized by severe hydronephrosis with progressive renal papillary atrophy and excessive volumes of dilute urine. Moreover, these mutant mice also showed a sodium-wasting phenotype, suggesting that *Hoxb7-CreMib1*$^{f/f}$ mice have defects in principal cells of the renal collecting duct. Using immunohistochemical staining, quantitative real-time RT-PCR, and transmission electron microscopy (TEM) analyses, we revealed that the *Hoxb7-CreMib1*$^{f/f}$ mouse renal collecting duct was composed predominantly of H^+-ATPase–expressing intercalated cells. Interestingly, introduction of the Notch intracellular domain (NICD) in the *Hoxb7-CreMib1*$^{f/f}$ mouse renal collecting duct completely reversed the altered cellular composition, and the entire collecting duct was composed of principal cells. These findings demonstrate that Mib1 regulates the Notch signaling pathway, which is required for the proper development of the mammalian renal collecting duct, especially the differentiation of epithelial precursor cells into principal cells.

Results

Disruption of Notch activation in the renal collecting duct of Hoxb7-CreMib1$^{f/f}$ *mice.* To first examine whether Notch signaling is involved in the mammalian renal collecting duct development, we performed immunohistochemical analyses using E16.5 C57BL/6 mouse embryonic kidneys. As previously reported (14, 15), Jag1 and Notch2 were expressed in various regions of the developing kidney, including the collecting duct (Figure 1, A and B). Interestingly, the fluorescent intensity of Jag1 in some collecting duct epithelial cells was higher than the intensity found in neighboring cells (Figure 1A, arrowhead). To examine the activation of Notch signaling in the developing renal collecting duct, we used transgenic Notch reporter (TNR) mice that distinctly express EGFP in

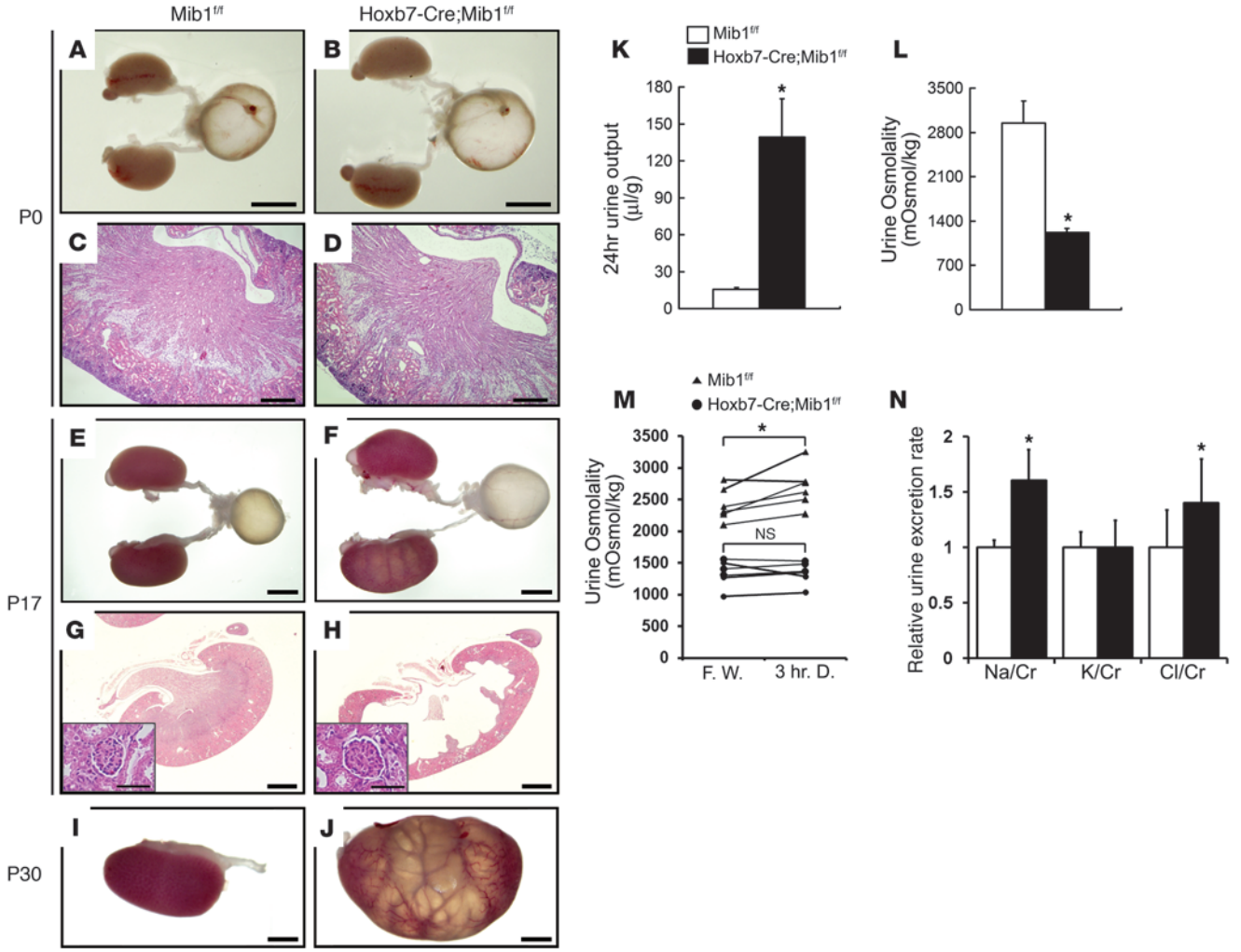

Figure 2

Progressive hydronephrosis, urinary concentrating defect, and sodium-wasting phenotype of *Hoxb7-CreMib1*$^{f/f}$ mice. (**A**–**H**) Urinary systems (**A**, **B**, **E**, and **F**) and H&E staining of kidneys (**C**, **D**, **G**, and **H**) from *Mib1*$^{f/f}$ (**A**, **C**, **E**, and **G**) and *Hoxb7-CreMib1*$^{f/f}$ (**B**, **D**, **F**, and **H**) littermates at P0 (**A**–**D**) or P17 (**E**–**H**). Scale bars: 2 mm (**A**, **B**, **E**, and **F**); 300 μm (**C** and **D**); 1 mm (**G** and **H**). High-magnification images of glomeruli are shown in insets in **G** and **H** (scale bars: 40 μm). (**I** and **J**) Kidneys of 1-month-old (P30) *Mib1*$^{f/f}$ (**I**) and *Hoxb7-CreMib1*$^{f/f}$ (**J**) littermates. Scale bars: 2 mm. (**K**) Urine output for 24 hours of 7-week-old *Mib1*$^{f/f}$ control and *Hoxb7-CreMib1*$^{f/f}$ mice. Error bars represent mean ± SD. **P* < 0.05. (**L**) Urine osmolality of 7-week-old *Mib1*$^{f/f}$ control and *Hoxb7-CreMib1*$^{f/f}$ mice. Error bars represent mean ± SD. **P* < 0.05. (**M**) Three-hour water deprivation test of 7-week-old *Mib1*$^{f/f}$ control and *Hoxb7-CreMib1*$^{f/f}$ mice. F.W., free access to water; 3 hr. D., 3-hour dehydration. **P* < 0.05 (paired *t* test). (**N**) Relative urinary excretion levels of indicated ions normalized to creatinine in 7-week-old *Mib1*$^{f/f}$ control and *Hoxb7-CreMib1*$^{f/f}$ mice. Error bars represent mean ± SD. **P* < 0.05.

cells with activated Notch/CBF-1 (30). In the renal collecting duct of a newborn TNR mouse, EGFP was mostly detected in the aquaporin-2–expressing (AQP2-expressing) cells but not in the AQP2-negative cells (Figure 1C, arrowheads), suggesting possible implication of Notch signaling in the differentiation and/or function of AQP2-expressing collecting duct epithelial cells. Mib1, an essential E3 ubiquitin ligase for the endocytosis of Notch ligands, was also expressed in various regions of the developing kidney, including the collecting duct (Figure 1D).

To elucidate the function of Notch signaling in the renal collecting duct development, we inactivated Mib1 in the renal collecting duct by crossing *Mib1*$^{f/f}$ mice, in which exons 2 and 3 of the *Mib1* gene are flanked by loxP sites (23, 26), with a transgenic mouse line that expresses Cre recombinase under the control of the Hoxb7 promoter (29). In the E18.5 *Hoxb7-CreMib1*$^{f/f}$ mouse embryos, Mib1 was specifically inactivated in the renal collecting duct but was retained in the other structures of nephron (Figure 1, E and F), which is consistent with the previous report that the Hoxb7-Cre transgenic mice specifically inactivate floxed genes along the collecting duct derived from ureteric bud (31, 32).

The interaction of Notch receptors with their ligands leads to sequential proteolytic cleavages of the Notch receptor, which results in the release of the NICD that translocates to the nucleus and turns on the Notch target genes. Western blot analysis revealed that the generation of cleaved Notch2 intracellular domain was markedly decreased in the *Hoxb7-CreMib1*$^{f/f}$ kidneys compared with

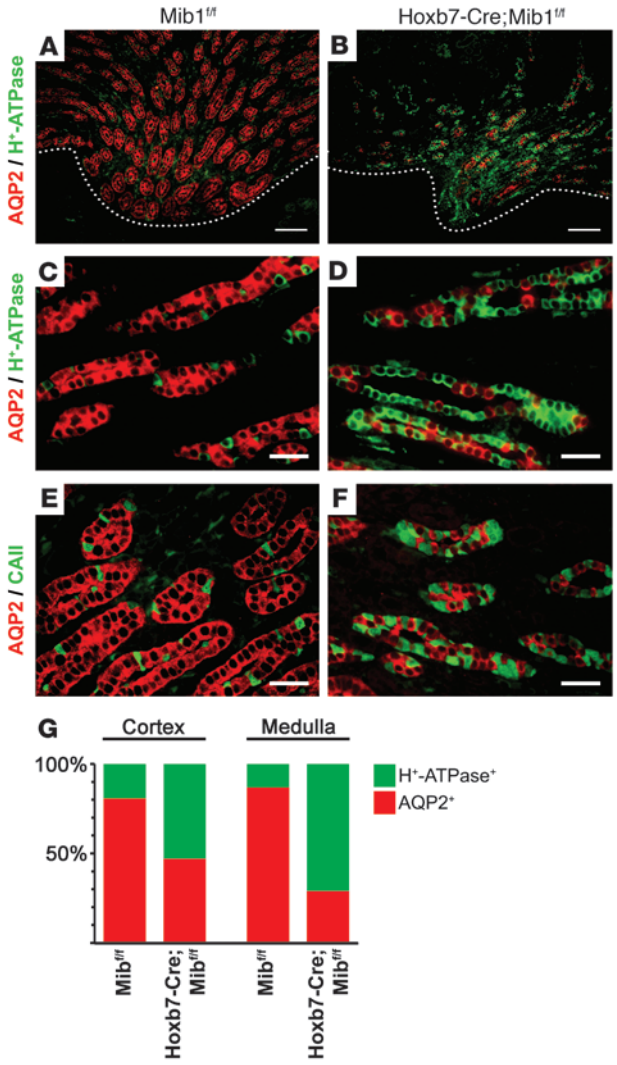

Figure 3
Altered cellular composition of the renal collecting duct in *Hoxb7-CreMib1$^{f/f}$* mice. (**A**–**F**) Immunohistochemical staining of medullary kidneys from P0 *Mib1$^{f/f}$* (**A**, **C**, and **E**) and *Hoxb7-CreMib1$^{f/f}$* (**B**, **D**, and **F**) littermates with anti-AQP2 (red), anti–H$^+$-ATPase (green, **A**–**D**), and anti-CAII (green, **E** and **F**) antibodies. Dotted lines indicate renal papilla. Scale bars: 50 μm (**A** and **B**); 30 μm (**C**–**F**). (**G**) Relative cell numbers of each cell type in the cortex and the medulla are compared.

WT (*Mib1$^{f/f}$*) littermates (Figure 1G). Among the various Notch target genes, only *Heyl* has been reported to be expressed in the developing renal collecting duct particularly, and other Notch target genes, such as *Hey1* and *Hey2* are not detected in this region (14). Quantitative real-time RT-PCR analysis showed that the expression of HeyL was significantly decreased in the medullary region of the kidney from E18.5 *Hoxb7-CreMib1$^{f/f}$* mouse embryos compared with that in WT littermates (Figure 1H). Taken together, these results show that the activation of Notch signaling is efficiently abrogated in the developing renal collecting duct of *Hoxb7-CreMib1$^{f/f}$* mice.

Severe hydronephrosis, urinary concentrating defect, and sodium-wasting phenotype in the Hoxb7-CreMib1$^{f/f}$ mice. The *Hoxb7-CreMib1$^{f/f}$* mice were born at the expected Mendelian ratio, viable to adulthood without external abnormalities, and fertile for several months. The urinary system in most of the P0 mutant mice appeared normal (Figure 2, A and B). However, all of the *Hoxb7-CreMib1$^{f/f}$* mice at P17 showed unilateral or bilateral hydronephrosis of distended kidneys (Figure 2, E and F), which became more severe at P30 (Figure 2, I and J). Histopathological analysis revealed that the kidneys of *Hoxb7-CreMib1$^{f/f}$* mice showed normal gross morphology and intact nephron structures at P0 (Figure 2, C and D, and Supplemental Figure 1; supplemental material available online with this article; doi:10.1172/JCI38416DS1) but became hydronephrotic with severe parenchymal atrophy, which was accompanied by severe dilatation of the pelvicaliceal system before 3 weeks of age; however, the renal cortex and glomerular structures were relatively well preserved (Figure 2, G and H).

To examine a functional defect of *Hoxb7-CreMib1$^{f/f}$* mouse kidneys, 24-hour urine samples were obtained by placing the mice in metabolic cages with ad libitum food and water access. As shown in Figure 2K, the *Hoxb7-CreMib1$^{f/f}$* mice exhibited an 8-fold increase in urine output compared with that in age-matched WT control mice (139.3 ± 31.1 μl/g of body weight for *Hoxb7-CreMib1$^{f/f}$* mice vs. 15.71 ± 1.34 μl/g of body weight for WT control mice; n = 5 per group). Consistently, urinary osmolality was markedly reduced in the *Hoxb7-CreMib1$^{f/f}$* mice (1,217 ± 62.1 mOsm/kg of H_2O for *Hoxb7-CreMib1$^{f/f}$* mice vs. 2,947 ± 346 mOsm/kg of H_2O for WT control mice; n = 5 per group; Figure 2L). The urinary osmolality remained unchanged even after 3 hours of water deprivation in mutant mice, while it concentrated significantly in WT control mice (Figure 2M). These results show that the *Hoxb7-CreMib1$^{f/f}$* mice have a severe urinary concentrating defect.

We next examined whether the *Hoxb7-CreMib1$^{f/f}$* mice have urinary sodium wasting, because the increase in urine output far exceeded the reduction fold of urinary osmolality in the mutant mice. As a result, the excretion rate of urinary sodium and chloride normalized with creatinine were increased in the *Hoxb7-CreMib1$^{f/f}$* mice compared with WT control mice (Figure 2N). Because both of the urinary concentration and sodium reabsorption are closely related with the functions of principal cells (31, 33), these results strongly suggest that inactivation of Notch signaling in the renal collecting duct may affect principal cells that lead to severe distal renal tubular defects.

Altered cellular composition in the Hoxb7-CreMib1$^{f/f}$ mouse renal collecting duct. The functional defects of *Hoxb7-CreMib1$^{f/f}$* mouse kidney might be due to an altered cellular composition in the renal collecting duct. To assess this possibility, we performed immunohistochemical staining with antibodies raised against AQP2 and H$^+$-ATPase as markers of the principal cells and intercalated cells, respectively. We examined very young newborn *Hoxb7-CreMib1$^{f/f}$* and WT littermates, before gross morphological changes of kidney had occurred. The renal collecting duct of newborn WT mice consisted of about 80% principal cells and 20% intercalated cells (80.75% ± 5.62% for principal cells vs. 19.25% ± 5.62% for intercalated cells in the cortical collecting duct, 86.84% ± 5.65% for principal cells vs. 13.16% ± 5.65% for intercalated cells in the medullary collecting duct; n = 4 per group; Figure 3, A, C, and G), which is similar to previous reports (7). However, the number of AQP2-expressing principal cells in the newborn *Hoxb7-CreMib1$^{f/f}$* mouse collecting duct was dramatically decreased, while the number of H$^+$-ATPase–expressing intercalated cells was markedly increased (47.05% ± 4.98% for principal cells vs. 52.95% ± 4.98% for intercalated cells in the cortical collecting duct, 29.01% ± 4.26% for prin-

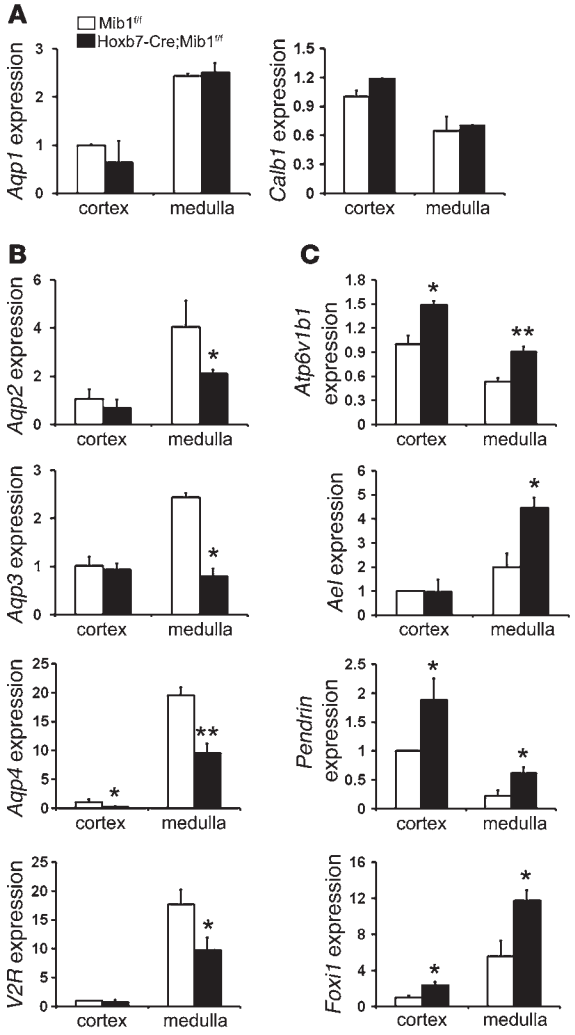

Figure 4
Quantitative real-time RT-PCR assays in the kidneys of P0 *Mib1*$^{f/f}$ and *Hoxb7-CreMib1*$^{f/f}$ littermates. (**A**) Analyses of AQP1 and Calbindin D-28k, which are not expressed in the collecting duct but expressed in proximal tubules and connecting tubules, respectively. (**B**) Analyses of principal cell–specific genes. (**C**) Analyses of intercalated cell–specific genes. At least 3 independent P0 *Mib1*$^{f/f}$ and *Hoxb7-CreMib1*$^{f/f}$ littermates were examined in 3 independent experiments, and representative results are shown. Error bars represent mean ± SD. $^{*}P < 0.05$, $^{**}P < 0.001$.

cipal cells vs. 70.99 ± 4.26% for intercalated cells in the medullary collecting duct; $n = 4$ per group; Figure 3, B, D, and G). Because the H^+-ATPase proteins can be expressed in the inner medullary collecting duct under special circumstances such as the AQP1 deficiency (34), we further confirmed that the H^+-ATPase–expressing cells, which were increased in number in the mutant renal collecting duct, are intercalated cells, by staining with antibody against CAII (35), another marker of intercalated cells (Figure 3, E and F).

Next, we performed quantitative real-time RT-PCR assays to measure the mRNA levels of principal cell– or intercalated cell–specific genes in the kidneys from P0 *Hoxb7-CreMib1*$^{f/f}$ and WT littermates. The AQP water channel proteins are expressed in the kidney at distinct sites and are essential for urinary concentration. AQP1 is extremely abundant in the proximal tubule and the descending thin limb, both structures derived from the metanephric mesenchyme, but is absent in the renal collecting duct (36). AQP2 is the predominant vasopressin-regulated water channel and is expressed exclusively in the principal cells of the connecting tubule and collecting duct (37). AQP3 (38) and AQP4 (39) are both present in the basolateral plasma membrane of the collecting duct principal cells and represent exit pathways for water reabsorbed apically via AQP2. AQP3 is very abundant in the connecting tubule as well as the cortical and medullary collecting duct, whereas AQP4 is abundant mainly in the inner medulla (39). First, we examined the mRNA levels of AQP1 (*Aqp1*) and Calbindin D-28k (*Calb1*), which are not expressed in the collecting ducts but in the proximal tubules and distal tubules, respectively. As a result, the mRNA levels between *Hoxb7-CreMib1*$^{f/f}$ and WT littermates were comparable, suggesting no apparent change in tubular structures of the mutant nephron (Figure 4A). However, the mRNA levels of AQP2 (*Aqp2*), AQP3 (*Aqp3*), and AQP4 (*Aqp4*) decreased significantly in the medullary region of the *Hoxb7-CreMib1*$^{f/f}$ mouse kidney (Figure 4B). The expression of vasopressin receptor type 2 (*V2R*) (40), another marker of principal cells, was also decreased in the *Hoxb7-CreMib1*$^{f/f}$ mouse kidneys compared with that in WT littermates (Figure 4B, bottom panel), indicating that the expression of all principal cell marker genes was decreased in the medulla of *Hoxb7-CreMib1*$^{f/f}$ kidneys.

The intercalated cells can be divided into at least 2 distinct cell types: α- and β-intercalated cells (41, 42). The α-intercalated cells are involved in proton secretion and are present in both the cortical and medullary collecting duct, while the β-intercalated cells take part in bicarbonate secretion and are found mainly in the cortical collecting duct (43). The α- and β-intercalated cells have 2 distinct anion exchangers, AE1 (44) and Pendrin (6), respectively. We found that the mRNA levels of α-intercalated cell marker *Ae1* and β-intercalated cell marker *Pendrin*, as well as H^+-ATPase (*Atp6v1b1*), increased in the *Hoxb7-CreMib1*$^{f/f}$ mouse kidney compared with that in WT littermates (Figure 4C). Moreover, the expression of the forkhead transcription factor *Foxi1*, which mediates the differentiation of intercalated cells (9), also increased markedly (Figure 4C, bottom panel).

To further reveal the identity of H^+-ATPase–expressing cells, which were increased in number in the newborn mutant collecting duct, we performed TEM analysis on the 3,3′-diaminobenzidine–stained (DAB-stained) sections of medullary renal collecting duct. As a result, the H^+-ATPase–expressing cells of the mutant renal collecting duct exhibited the characteristics of intercalated cells (45), such as microvillous apex, plenty of granules and mitochondria, and dark-staining cytoplasms (Figure 5). Taken together, these data show that the inactivation of Notch signaling in renal collecting duct causes the alteration of cellular composition during development and suggest the possibility that Notch signaling regulates the differentiation of principal cells.

The distal renal tubular defects of Hoxb7-CreMib1$^{f/f}$ *mice are due to altered differentiation of principal cells.* According to the previous reports, dietary lithium treatment can downregulate the expressions of AQP2 and AQP3 as well as other proteins involved in sodium and water reabsorption in rats (46, 47), which coincided with an increased ratio of intercalated cells to principal cells in the collecting duct (48, 49). These reports suggest that remodeling of renal collecting duct can occur for the physiological adaptation to various abnormal conditions. Thus, to exclude the possibility that the phenotype of mutant renal collecting duct is an indirect effect of hydronephrosis after birth, we examined the cellular composi-

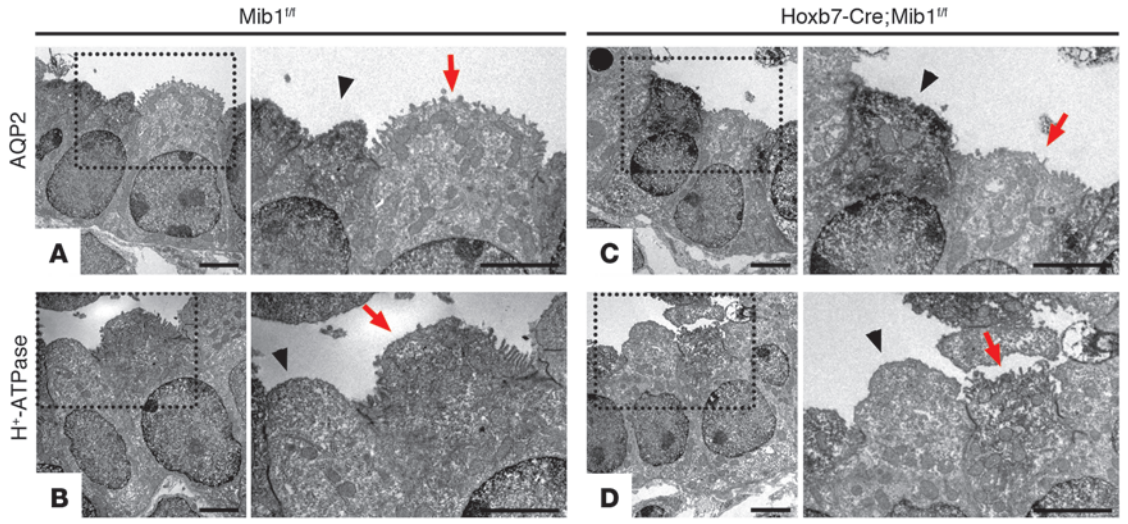

Figure 5
TEM analysis on DAB-stained sections of the medullary collecting duct. Sections from P0 *Mib1*$^{f/f}$ (**A** and **B**) and *Hoxb7-CreMib1*$^{f/f}$ (**C** and **D**) littermates were stained with anti-AQP2 (**A** and **C**) or anti–H$^+$-ATPase (**B** and **D**) antibodies. The panels in the second and fourth columns are high-magnification images of the areas in the dotted squares. Black arrowheads and red arrows indicate the AQP2-labeled cells and H$^+$-ATPase–labeled cells, respectively. Scale bars: 3 μm.

tion of renal collecting duct from E18.5 mouse embryos. We found that the *Hoxb7-CreMib1*$^{f/f}$ mouse embryos already had altered cellular composition of decreased principal cells and increased intercalated cells in renal collecting duct, suggesting that disrupted differentiation of principal cells is the direct effect of Mib1 deletion in the renal collecting duct (Figure 6, A–D). Intriguingly, the H$^+$-ATPase proteins showed abnormal cytoplasmic accumulation in the mutant intercalated cells, while they were mainly localized in the apical membrane of WT intercalated cells (Figure 6B).

Defective pyeloureteral peristalsis can cause progressive renal obstruction, severe hydronephrosis, and, eventually, fatal renal failure (50). Because the Hoxb7-Cre transgenic mouse line also deletes floxed genes in ureteral epithelium, we investigated whether the development of ureter in the P0 *Hoxb7-CreMib1*$^{f/f}$ mice was affected. H&E staining showed that the *Hoxb7-CreMib1*$^{f/f}$ mice had normal morphology of ureter (Figure 6, E and F), and layers of smooth muscle cells were developed normally compared with those in WT littermates (Figure 6, G and H), indicating that Mib1 is dispensable for the development of ureter and that renal defects of the *Hoxb7-CreMib1*$^{f/f}$ mice are not due to defective ureteral development.

Because Mib1 can interact not only with Notch ligands but also the substrate DAPK, which mediates caspase-dependent apoptotic cell death (51), we investigated whether the inactivation of Mib1 affects the apoptosis of renal collecting duct epithelial cells. Immunohistochemical staining with anti-active Caspase-3 antibody revealed no apparent apoptotic cells in the renal collecting ducts of E18.5 *Hoxb7-CreMib1*$^{f/f}$ mouse embryos as well as WT littermates (Figure 6, I and J), implying that Mib1 deletion does not cause aberrant apoptosis of specific cell types.

The principal cell differentiation is positively regulated by Notch signaling in the renal collecting duct. We further examined whether the phenotypic changes in the *Hoxb7-CreMib1*$^{f/f}$ mice are caused entirely by defective Notch signaling. To compensate for the Mib1 deletion and activate Notch signaling in the renal collecting duct, we bred the *Hoxb7-CreMib1*$^{f/f}$ mice with Rosa-NICD transgenic mice (52). In the *Hoxb7-CreMib1*$^{f/f}$*Rosa-NICD* mice, the NICD is expressed in the Mib1-deleted renal collecting duct and activates the Notch signaling constitutively. Intriguingly, the altered cellular composition of renal collecting duct shown in the *Hoxb7-CreMib1*$^{f/f}$ mice was completely reversed in the newborn *Hoxb7-CreMib1*$^{f/f}$*Rosa-NICD* mouse kidneys; the whole renal collecting duct of the *Hoxb7-CreMib1*$^{f/f}$ *Rosa-NICD* mouse was made up of AQP2-expressing principal cells. In addition, the expression of intercalated cell markers H$^+$-ATPase and CAII was completely absent in the cortical and medullary collecting ducts (Figure 7, A–I). Recently, epithelial precursor cells in the renal collecting duct were reported to express both AQP2 and CAII (9), but no accumulation of such undifferentiated precursor cells in the *Hoxb7-CreMib1*$^{f/f}$*Rosa-NICD* mouse kidneys was found. Quantitative real-time RT-PCR analyses showed that the expression of *Heyl* and *Aqp2* were dramatically increased in the *Hoxb7-CreMib1*$^{f/f}$*Rosa-NICD* mouse kidney compared with that in WT littermates, whereas the expression of *Atp6v1b1* was markedly decreased (Figure 7J). These results show that the activation of Notch signaling in the developing renal collecting duct is critical for the differentiation of precursor cells into principal cells and that impaired differentiation into principal cells in the Mib1-inactivated collecting duct is due to defective Notch signaling.

Discussion

It is well known that proximal nephron development of the mammalian kidney, which is derived from metanephric mesenchyme, requires activation of the Notch signaling pathway (2). However, the function and importance of Notch signaling in the development of the renal collecting duct, which is derived from the ureteric bud, have not been investigated. Here, we show that Mib1 deficiency in the developing renal collecting duct results in the inactivation of Notch signaling, which causes aberrant differentiation to principal cells. The decrease of principal cells leads to urinary concentrating defect and sodium-wasting phenotype in the mutant mice, resulting in excessive volumes of hypotonic urine

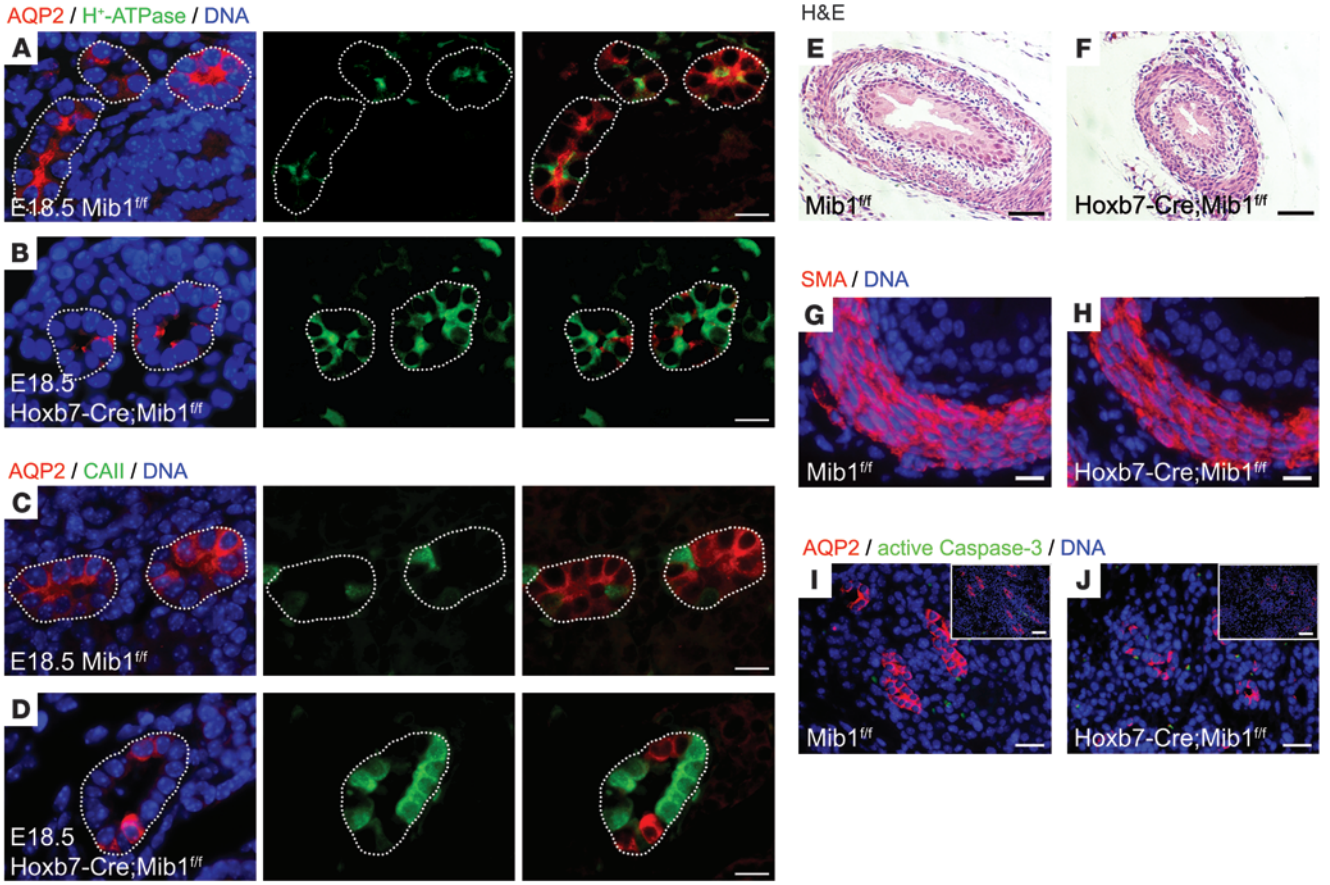

Figure 6
Altered cellular composition of *Hoxb7-CreMib1*$^{f/f}$ mouse kidneys is the primary phenotype of the collecting duct–specific Mib1 deletion. (**A**–**D**) Immunohistochemical staining of embryonic kidneys from E18.5 *Mib1*$^{f/f}$ (**A** and **C**) and *Hoxb7-CreMib1*$^{f/f}$ (**B** and **D**) littermates with anti-AQP2 (red, **A** and **B**), anti-CAII (green, **C** and **D**), and anti–H$^+$-ATPase (green, **A**–**D**) antibodies. Hoechst (blue) stains DNA, and dotted lines indicate renal collecting ducts. Scale bars: 15 μm. (**E** and **F**) H&E staining of ureters from P0 *Mib1*$^{f/f}$ (**E**) and *Hoxb7-CreMib1*$^{f/f}$ (**F**) littermates. Scale bars: 30 μm. (**G** and **H**) Immunohistochemical staining of ureters from P0 *Mib1*$^{f/f}$ (**G**) and *Hoxb7-CreMib1*$^{f/f}$ (**H**) littermates with anti–α-SMA antibody (red). Hoechst (blue) stains DNA. Scale bars: 15 μm. (**I** and **J**) Immunohistochemical staining of embryonic kidneys from E18.5 *Mib1*$^{f/f}$ (**I**) and *Hoxb7-CreMib1*$^{f/f}$ (**J**) littermates with anti-AQP2 (red) and anti-active Caspase-3 (green) antibodies. Hoechst (blue) stains DNA. Low-magnification images are shown in insets. Scale bars: 25 μm.

and severe hydronephrosis. These results demonstrate that Notch signaling is required for the development of a ureteric bud into the functional mammalian renal collecting duct and is especially important for the differentiation of precursor cells into principal cells. In addition, we believe our study is the first report to provide direct evidence that renal collecting duct dysplasia can cause nephrogenic diabetes insipidus.

In the mature nephron, functionally distinct cell types are typically arranged in discrete tubule segments that process filtered blood sequentially, as it passes through the nephron. However, intercalated cells and principal cells are intermingled in the renal collecting duct, and the proper differentiation of these cell types is critical to ensure accurate functioning of the collecting duct, including the regulation of fluid, electrolytes, and acid-base homeostasis (53). A recent study with mice lacking Foxi1 suggested that Foxi1 is required for the differentiation of precursor cells into intercalated cells and that Foxi1 regulates the expression of intercalated cell–specific genes, *AE1* and *Pendrin* (9). Nevertheless, the molecular mechanisms that regulate principal cell differentiation are unclear. In our present study, activation and inactivation of Notch signaling in the renal collecting duct led to predominant differentiation of precursor cells into principal cells and intercalated cells, respectively, suggesting that the alternative cell fate choice of these principal and intercalated cells is dependent on Notch signaling. Our results are consistent with previous studies that suggest that principal cells and intercalated cells arise from a common progenitor cell (54–56). Moreover, because the introduction of NICD was sufficient for the differentiation of all renal collecting duct epithelium into principal cells, Notch signaling might inhibit the function of Foxi1 directly or indirectly for the proper differentiation into principal cells.

During embryonic kidney development, both Jag1 and Notch2 are expressed in the collecting duct epithelia. However, EGFP proteins in the TNR transgenic mouse kidneys were expressed in the AQP2-expressing cells exclusively, implying that Notch signaling is activated only in the principal cells. These findings are consistent with the results indicating that Notch signaling is required for differentiation into principal cells. In various vertebrate tissues, such

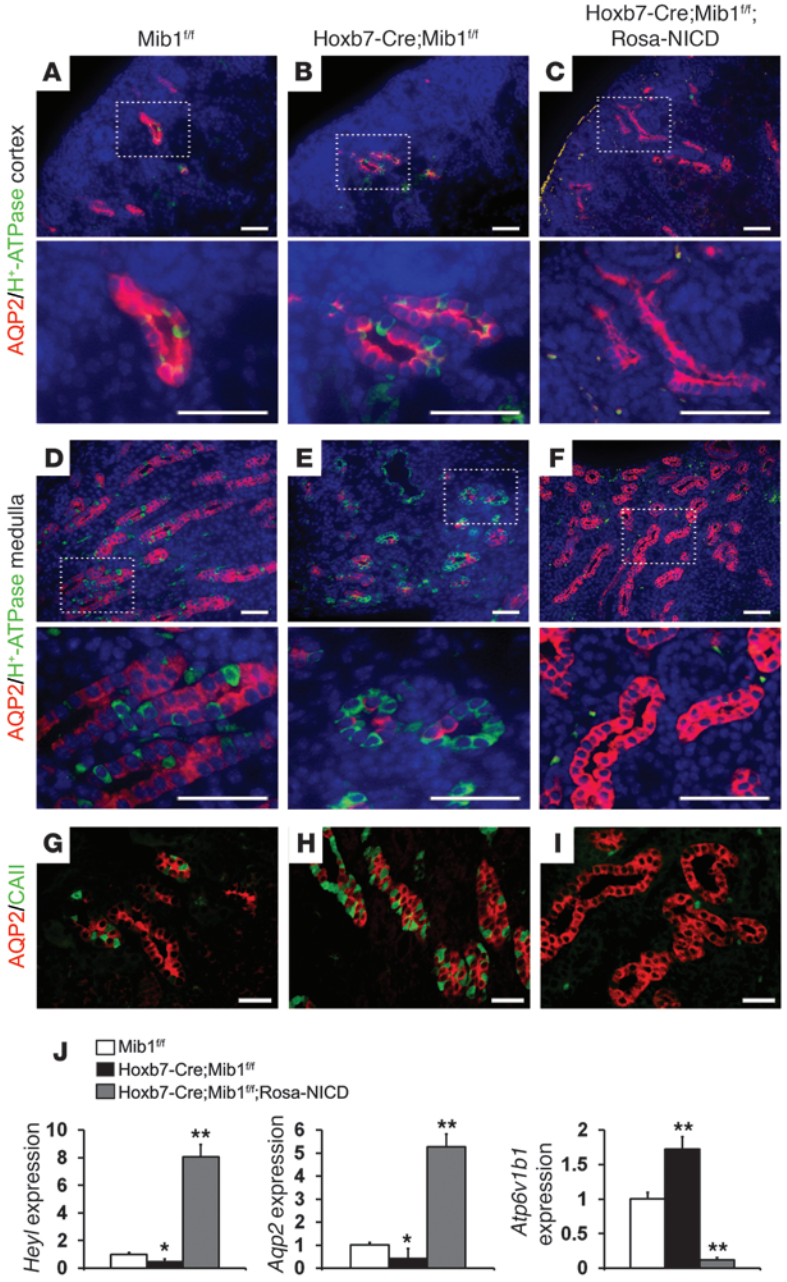

Figure 7
The phenotype of *Hoxb7-CreMib1*$^{f/f}$ mouse kidney is reversed by constitutively activated Notch signaling. (**A**–**F**) Immunohistochemical staining with anti-AQP2 (red) and anti–H$^+$-ATPase (green) antibodies in sections of kidney cortex (**A**–**C**) and medulla (**D**–**F**) from P0 *Mib1*$^{f/f}$ (**A** and **D**), *Hoxb7-CreMib1*$^{f/f}$ (**B** and **E**), and *Hoxb7-CreMib1*$^{f/f}$*Rosa-NICD* (**C** and **F**) littermates. Hoechst (blue) stains the nuclei. Scale bars: 50 μm. High-magnification images of the boxed regions in the first and third rows are shown in the second and fourth rows, respectively. (**G**–**I**) Immunohistochemical staining with anti-AQP2 (red) and anti-CAII (green) antibodies in medullary kidneys from P0 *Mib1*$^{f/f}$ (**G**), *Hoxb7-CreMib1*$^{f/f}$ (**H**), and *Hoxb7-CreMib1*$^{f/f}$*Rosa-NICD* (**I**) littermates. Scale bars: 30 μm. (**J**) Quantitative real-time RT-PCR analyses of indicated genes in the kidneys from P0 *Mib1*$^{f/f}$, *Hoxb7-CreMib1*$^{f/f}$, and *Hoxb7-CreMib1*$^{f/f}$*Rosa-NICD* littermates. Error bars represent mean ± SD. $^*P < 0.05$, $^{**}P < 0.001$.

as brain (57), inner ear (58), skeletal muscle (59, 60), bone marrow (61, 62), and intestine (63, 64), Notch signaling is transduced by the lateral inhibition mechanism during cell fate determination. Our data show that the mammalian renal collecting duct is another example of a tissue that adopts Notch-regulated lateral inhibition to achieve cell type specification.

Although Notch signaling is required to produce the heterogeneous cellular composition of principal cells and intercalated cells in the renal collecting duct, the differentiation into principal cells was not blocked completely and the severities of the phenotypes were different between the cortical and medullary collecting duct in the *Hoxb7-CreMib1*$^{f/f}$ mice. This suggested several possibilities: (a) mosaicism of Cre recombinase expression in the Hoxb7-Cre transgenic mouse line causes incomplete loss of Mib1 in renal collecting duct; (b) AQP2-expressing cells in mutant kidneys are not mature principal cells but undifferentiated precursor cells; and/or (c) not only Mib1 but also other factors participate in the differentiation of collecting duct epithelium. First, according to previous studies with Rosa26 reporter system (29, 31) and our data, there is no evidence of mosaicism in Cre activity of Hoxb7-Cre mice. Of particular importance, complete extinction of intercalated cells in the *Hoxb7-CreMib*$^{f/f}$ *Rosa-NICD* mouse kidneys showed efficient gene recombination by Cre along the entire collecting duct, suggesting that this is not likely to be the case. Second, the remaining AQP2-expressing cells in the *Hoxb7-CreMib1*$^{f/f}$ mouse kidneys were not proliferative (data not shown) and were not labeled with CAII or other intercalated cell markers; thus, as above, this cannot be a proper explanation. Third, the most probable explanation for the incomplete loss of principal cells in the *Hoxb7-CreMib1*$^{f/f}$ mouse kidney is that other factors are involved in the process of collecting duct maturation. For example, Mib2, a paralog of Mib1, is likely to have redundant function of Mib1 in the developing kidney (22). Indeed, the mRNA level of *Mib2* was rather increased in the *Hoxb7-CreMib1*$^{f/f}$ mouse kidney (data not shown). Further studies will be needed to determine molecular mechanisms and processes of the principal cell differentiation.

Recent studies with various mouse models of AQP2 conditional knockout or mutations have reported that polyurea alone can cause severe hydronephrosis (65–67). For example, Lloyd and his colleagues reported that mice with an F204V mutation in the *Aqp2* gene develop severe hydronephrosis as well as nephrogenic diabetes insipidus (65). Similarly, McDill and his colleagues showed that a single-base mutation in codon 256 of *Aqp2* gene causes a Ser to Leu substitution, loss of Aqp2 phosphorylation at amino acid 256, and the absence of apical accumulation of the protein. These mutant mice have no response to a vasopressin analog and produce large quantities of hypotonic urine, resulting in the severe hydronephrosis, obstructive nephropathy, renal failure, and death (66). In the collecting duct–specific AQP2 conditional knockout mice, using the

same Hoxb7-Cre transgenic mice that we used for this study, the kidneys showed progressive papillary atrophy and hydronephrosis. Collectively, like other mouse models of nephrogenic diabetes insipidus, the severe hydronephrosis of *Hoxb7-CreMib1$^{f/f}$* mice is presumably a consequence of an inability to cope with the extreme polyuria caused by altered principal cell differentiation, rather than obstruction of the lower urinary track or other unknown phenotypes.

Recently, the Notch signaling pathway was shown to be activated in rat kidney after acute ischemic injury (68). The recovery from acute kidney injury requires the replacement of damaged cells with new cells to restore the integrity of the tubular epithelium. Previous reports have revealed that renal regeneration processes may redeploy certain parts of the genetic program executed during organogenesis to reestablish proper tissue function in the kidney (69, 70). Here, we would like to point out the definitive role of Notch signaling not only in the proximal region but also in the collecting duct during kidney development. Therefore, the regulation of Notch signaling in various regions might be able to pave the way for the repair of the entire mammalian kidney.

Methods

Mice. Floxed Mib1 (*Mib1$^{f/f}$*) mice were generated as described previously (23). The Hoxb7-Cre transgenic mice were purchased from The Jackson Laboratory. Rosa-NICD and TNR mice were gifts from D. Melton (Harvard University, Boston, Massachusetts, USA) and N. Gaiano (Johns Hopkins University, Baltimore, Maryland, USA), respectively. We bred *Hoxb7-CreMib1$^{f/f}$* mice with *Mib1$^{f/f}$* mice for the most of the experiments or with Mib1 homozygous Rosa-NICD transgenic mice (*Mib1$^{f/f}$Rosa-NICD*) for the rescue experiment and examined the pups. All mouse lines were bred onto a C57BL/6 background (backcrossed for more than 7 generations) and maintained in specific pathogen–free conditions at the POSTECH animal facility. All animal experiments were approved by the ethical committees at POSTECH.

Histology, immunohistochemistry, and Western blot analysis. The mouse kidney tissues were fixed in 4% paraformaldehyde overnight at 4°C, paraffin embedded, sectioned (thickness, 4 μm), and stained with H&E. Paraffin sections were incubated with rabbit anti-Mib1 (a gift from J. Peng, Emory University, Atlanta, Georgia, USA); goat anti-AQP2, rabbit anti-H^+-ATPase, and mouse anti-CAII (Santa Cruz Biotechnology Inc.); mouse anti-SMA (Neomarkers); and/or rabbit anti-active Caspase-3 (BD Biosciences — Pharmingen) antibodies and then were visualized with Alexa 488– or Alexa 594–conjugated secondary antibodies (Invitrogen). Newborn mouse kidneys were prepared and visualized as described in Supplemental Methods. For frozen sections, embryonic and newborn mouse kidney tissues were fixed in 4% paraformaldehyde for 2 hours at 4°C and embedded in an optimal-cutting-temperature compound for sectioning (thickness, 15 μm). Frozen sections were immunostained with rabbit anti-Jag1 and rabbit anti-Notch2 (Santa Cruz Biotechnology Inc.) and/or rabbit anti-EGFP (Invitrogen) antibodies. Protein extraction and Western blot analyses were performed as described previously (21). Rabbit anti-activated Notch2 antibody (Abcam) was used.

Urine measurements. Twenty-four-hour urine samples were obtained by placing the mice in specially designed mini-metabolic cages (Natsume Seisakusho), which register urine volume and measure urine osmolarity (Vapro 5520; Wescor). Three-hour urine samples were obtained from mice with no access to the water (water deprivation hours, 8:00 AM ~ 11:00 AM). Control 3-hour urine samples were obtained from the same mice, on a subsequent day when mice had free access to water (n = 6 per group).

TEM. Sections of 2% paraformaldehyde-lysine-periodate–fixed (PLP-fixed) tissue were cut at 50 μm transversely through the kidney, using a vibratome, and were processed for immunohistochemistry, using an indirect immunoperoxidase method. All sections were washed 3 times for 15 minutes in PBS containing 50 mM NH_4Cl. Before incubation with the primary antibodies, the sections were incubated for 4 hours with PBS containing 1% BSA, 0.05% saponin, and 0.2% gelatin (solution A). The tissue sections were then incubated overnight at 4°C, with antibodies directed against H^+-ATPase (1:1,000) or AQP2 (1:800) diluted in solution A. After several washes in PBS containing 0.1% BSA, 0.05% saponin, and 0.2% gelatin (solution B), the tissue sections were incubated for 2 hours in horseradish peroxidase–conjugated donkey anti-rabbit IgG FaB fragment (Jackson ImmunoResearch Laboratories Inc.) diluted 1:100 in PBS containing 1% BSA (solution C). The tissues were then rinsed, first in solution B and then in 0.05 M Tris buffer (pH 7.6). To detect horseradish peroxidase, the sections were incubated in 0.1% DAB in 0.05 M Tris buffer for 5 minutes. Then, H_2O_2 was added to a final concentration of 0.01%, and the incubation was continued for 10 minutes. The sections were washed 3 times with 0.05 M Tris buffer and postfixed with 1% glutaraldehyde and 1% osmium tetroxide in 0.1 M phosphate buffer, before being dehydrated and mounted in Poly/Bed 812 resin (Polysciences) between polyethylene vinyl sheets. Ultrathin sections were stained with uranyl acetate and photographed using a transmission electron microscope (JEOL 1200EX).

Morphometric analysis. The number of specific marker-labeled cells in the cortex and medulla was counted. In a view field at a magnification of ×200 (in cortex) or ×400 (in medulla), the total number of cells in the AQP2-stained collecting ducts was counted using the nuclear stain, Hoechst 33342 (Invitrogen), and the number of AQP2-expressing cells and H^+-ATPase–expressing cells were counted. The cells in at least 25 tubuli of the cortex and 40 tubuli in the medulla were counted for each animal. Three WT and three *Hoxb7-CreMib1$^{f/f}$* mouse kidneys from separate animals were used.

Quantitative real-time RT-PCR. Newborn mouse kidney tissues were dissected into the cortical and medullary fractions and RNAs were extracted using the RNeasy Micro kit (Qiagen) according to the manufacturer's instructions. The RNAs were converted into cDNAs using the Omniscript kit (Qiagen). Quantification of cDNAs from specific mRNA transcripts was accomplished by quantitative real-time RT-PCR (Bio-Rad) using SYBR Green technology (Quantitect SYBR Green PCR kit; QIAGEN) as described previously (71). β-Actin was used as an internal control. Primer sequences are shown in Supplemental Table 1.

Statistics. All values are given as mean ± SD. Statistical comparisons were made by 2-tailed Student's t test. For the water deprivation test, 2-tailed paired Student's t test was used. A P value of less than 0.05 was considered to be statistically significant.

Acknowledgments

We thank the members of Y.-Y. Kong's lab for helpful discussions; J.K. Han, T.H. Kwon, and K.H. Han for expert comments; M.P. Kong and H.S. Hwang for technical support; and N. Gaiano and D.A. Melton for provision of materials. This work was supported by grants from the Center for Biological Modulators of the 21C Frontier R&D Program (CBM32-A2300-01-00-01); the National R&D Program for Cancer Control, Ministry of Health and Welfare, Republic of Korea (0920310); the Korea Science and Engineering Foundation (2009-0062785); and Basic Science Research Program through the National Research Foundation of Korea (2009-0079371), funded by the Ministry of Education, Science, and Technology.

Received for publication December 22, 2008, and accepted in revised form August 26, 2009.

Address correspondence to: Young-Yun Kong, Department of Biological Sciences, Seoul National University, 599 Gwanak-ro, Gwanak-gu, Seoul, 151-747, Republic of Korea. Phone: 82-2-880-2638; Fax: 82-2-872-1993; E-mail: ykong@snu.ac.kr.

1. Bates, C.M. 2005. Transcriptional control of renal collecting duct development. *Am. J. Physiol. Renal Physiol.* **288**:F897–F898.
2. Dressler, G.R. 2006. The cellular basis of kidney development. *Annu. Rev. Cell Dev. Biol.* **22**:509–529.
3. Yu, J., McMahon, A.P., and Valerius, M.T. 2004. Recent genetic studies of mouse kidney development. *Curr. Opin. Genet. Dev.* **14**:550–557.
4. Burrow, C.R. 2000. Regulatory molecules in kidney development. *Pediatr. Nephrol.* **14**:240–253.
5. Wagner, C.A., and Geibel, J.P. 2002. Acid-base transport in the collecting duct. *J. Nephrol.* **15**(Suppl. 5):S112–S127.
6. Kim, Y.H., et al. 2002. Immunocytochemical localization of pendrin in intercalated cell subtypes in rat and mouse kidney. *Am. J. Physiol. Renal Physiol.* **283**:F744–F754.
7. Song, H.K., et al. 2007. Origin and fate of pendrin-positive intercalated cells in developing mouse kidney. *J. Am. Soc. Nephrol.* **18**:2672–2682.
8. Woolf, A.S., Price, K.L., Scambler, P.J., and Winyard, P.J. 2004. Evolving concepts in human renal dysplasia. *J. Am. Soc. Nephrol.* **15**:998–1007.
9. Blomqvist, S.R., et al. 2004. Distal renal tubular acidosis in mice that lack the forkhead transcription factor Foxi1. *J. Clin. Invest.* **113**:1560–1570.
10. Bray, S.J. 2006. Notch signalling: a simple pathway becomes complex. *Nat. Rev. Mol. Cell Biol.* **7**:678–689.
11. Cheng, H.T., et al. 2003. Gamma-secretase activity is dispensable for mesenchyme-to-epithelium transition but required for podocyte and proximal tubule formation in developing mouse kidney. *Development.* **130**:5031–5042.
12. Wang, P., Pereira, F.A., Beasley, D., and Zheng, H. 2003. Presenilins are required for the formation of comma- and S-shaped bodies during nephrogenesis. *Development.* **130**:5019–5029.
13. Cheng, H.T., et al. 2007. Notch2, but not Notch1, is required for proximal fate acquisition in the mammalian nephron. *Development.* **134**:801–811.
14. Leimeister, C., Schumacher, N., and Gessler, M. 2003. Expression of Notch pathway genes in the embryonic mouse metanephros suggests a role in proximal tubule development. *Gene Expr. Patterns.* **3**:595–598.
15. McCright, B., et al. 2001. Defects in development of the kidney, heart and eye vasculature in mice homozygous for a hypomorphic Notch2 mutation. *Development.* **128**:491–502.
16. Pavlopoulos, E., et al. 2001. neuralized Encodes a peripheral membrane protein involved in delta signaling and endocytosis. *Dev. Cell.* **1**:807–816.
17. Itoh, M., et al. 2003. Mind bomb is a ubiquitin ligase that is essential for efficient activation of Notch signaling by Delta. *Dev. Cell.* **4**:67–82.
18. Ruan, Y., Tecott, L., Jiang, M.M., Jan, L.Y., and Jan, Y.N. 2001. Ethanol hypersensitivity and olfactory discrimination defect in mice lacking a homolog of Drosophila neuralized. *Proc. Natl. Acad. Sci. U. S. A.* **98**:9907–9912.
19. Vollrath, B., Pudney, J., Asa, S., Leder, P., and Fitzgerald, K. 2001. Isolation of a murine homologue of the Drosophila neuralized gene, a gene required for axonemal integrity in spermatozoa and terminal maturation of the mammary gland. *Mol. Cell. Biol.* **21**:7481–7494.
20. Song, R., et al. 2006. Neuralized-2 regulates a Notch ligand in cooperation with Mind bomb-1. *J. Biol. Chem.* **281**:36391–36400.
21. Koo, B.K., et al. 2005. Mind bomb 1 is essential for generating functional Notch ligands to activate Notch. *Development.* **132**:3459–3470.
22. Koo, B.K., et al. 2005. Mind bomb-2 is an E3 ligase for Notch ligand. *J. Biol. Chem.* **280**:22335–22342.
23. Koo, B.K., et al. 2007. An obligatory role of mind bomb-1 in notch signaling of mammalian development. *PLoS ONE.* **2**:e1221.
24. Song, R., et al. 2008. Mind bomb 1 in the lymphopoietic niches is essential for T and marginal zone B cell development. *J. Exp. Med.* **205**:2525–2536.
25. Kim, Y.W., et al. 2008. Defective Notch activation in microenvironment leads to myeloproliferative disease. *Blood.* **112**:4628–4638.
26. Yoon, K.J., et al. 2008. Mind bomb 1-expressing intermediate progenitors generate notch signaling to maintain radial glial cells. *Neuron.* **58**:519–531.
27. Koo, B.K., et al. 2009. Notch signaling promotes the generation of EphrinB1-positive intestinal epithelial cells. *Gastroenterology.* **137**:145–155, 155.e1–155.e3.
28. Yoon, M.J., et al. 2008. Mind bomb-1 is essential for intraembryonic hematopoiesis in the aortic endothelium and the subaortic patches. *Mol. Cell. Biol.* **28**:4794–4804.
29. Yu, J., Carroll, T.J., and McMahon, A.P. 2002. Sonic hedgehog regulates proliferation and differentiation of mesenchymal cells in the mouse metanephric kidney. *Development.* **129**:5301–5312.
30. Mizutani, K., Yoon, K., Dang, L., Tokunaga, A., and Gaiano, N. 2007. Differential Notch signalling distinguishes neural stem cells from intermediate progenitors. *Nature.* **449**:351–355.
31. Rubera, I., et al. 2003. Collecting duct-specific gene inactivation of alphaENaC in the mouse kidney does not impair sodium and potassium balance. *J. Clin. Invest.* **112**:554–565.
32. Olsen, O., et al. 2007. Renal defects associated with improper polarization of the CRB and DLG polarity complexes in MALS-3 knockout mice. *J. Cell Biol.* **179**:151–164.
33. Loffing, J., et al. 2001. Aldosterone induces rapid apical translocation of ENaC in early portion of renal collecting system: possible role of SGK. *Am. J. Physiol. Renal Physiol.* **280**:F675–F682.
34. Kim, Y.H., Kim, J., Verkman, A.S., and Madsen, K.M. 2003. Increased expression of H+-ATPase in inner medullary collecting duct of aquaporin-1-deficient mice. *Am. J. Physiol. Renal Physiol.* **285**:F550–F557.
35. Breton, S., et al. 1995. Depletion of intercalated cells from collecting ducts of carbonic anhydrase II-deficient (CAR2 null) mice. *Am. J. Physiol.* **269**:F761–F774.
36. Nielsen, S., Smith, B.L., Christensen, E.I., Knepper, M.A., and Agre, P. 1993. CHIP28 water channels are localized in constitutively water-permeable segments of the nephron. *J. Cell Biol.* **120**:371–383.
37. Fushimi, K., et al. 1993. Cloning and expression of apical membrane water channel of rat kidney collecting tubule. *Nature.* **361**:549–552.
38. Ecelbarger, C.A., et al. 1995. Aquaporin-3 water channel localization and regulation in rat kidney. *Am. J. Physiol.* **269**:F663–F672.
39. Terris, J., Ecelbarger, C.A., Marples, D., Knepper, M.A., and Nielsen, S. 1995. Distribution of aquaporin-4 water channel expression within rat kidney. *Am. J. Physiol.* **269**:F775–F785.
40. Birnbaumer, M., et al. 1992. Molecular cloning of the receptor for human antidiuretic hormone. *Nature.* **357**:333–335.
41. Bastani, B., Yang, L., and Steinhardt, G. 1994. Immunocytochemical localization of vacuolar H-ATPase in the opossum (Monodelphis domestica) kidney: comparison with the rat. *J. Am. Soc. Nephrol.* **4**:1558–1563.
42. Bastani, B. 1997. Immunocytochemical localization of the vacuolar H(+)-ATPase pump in the kidney. *Histol. Histopathol.* **12**:769–779.
43. Batlle, D., Ghanekar, H., Jain, S., and Mitra, A. 2001. Hereditary distal renal tubular acidosis: new understandings. *Annu. Rev. Med.* **52**:471–484.
44. Sabolic, I., Brown, D., Gluck, S.L., and Alper, S.L. 1997. Regulation of AE1 anion exchanger and H(+)-ATPase in rat cortex by acute metabolic acidosis and alkalosis. *Kidney Int.* **51**:125–137.
45. Kaissling, B., and Kriz, W. 1979. Structural analysis of the rabbit kidney. *Adv. Anat. Embryol. Cell Biol.* **56**:1–123.
46. Kwon, T.H., et al. 2000. Altered expression of renal AQPs and Na(+) transporters in rats with lithium-induced NDI. *Am. J. Physiol. Renal Physiol.* **279**:F552–F564.
47. Marples, D., Christensen, S., Christensen, E.I., Ottosen, P.D., and Nielsen, S. 1995. Lithium-induced downregulation of aquaporin-2 water channel expression in rat kidney medulla. *J. Clin. Invest.* **95**:1838–1845.
48. Christensen, B.M., et al. 2004. Changes in cellular composition of kidney collecting duct cells in rats with lithium-induced NDI. *Am. J. Physiol. Cell Physiol.* **286**:C952–C964.
49. Kim, Y.H., et al. 2003. Altered expression of renal acid-base transporters in rats with lithium-induced NDI. *Am. J. Physiol. Renal Physiol.* **285**:F1244–F1257.
50. Chang, C.P., et al. 2004. Calcineurin is required in urinary tract mesenchyme for the development of the pyeloureteral peristaltic machinery. *J. Clin. Invest.* **113**:1051–1058.
51. Jin, Y., Blue, E.K., Dixon, S., Shao, Z., and Gallagher, P.J. 2002. A death-associated protein kinase (DAPK)-interacting protein, DIP-1, is an E3 ubiquitin ligase that promotes tumor necrosis factor-induced apoptosis and regulates the cellular levels of DAPK. *J. Biol. Chem.* **277**:46980–46986.
52. Murtaugh, L.C., Stanger, B.Z., Kwan, K.M., and Melton, D.A. 2003. Notch signaling controls multiple steps of pancreatic differentiation. *Proc. Natl. Acad. Sci. U. S. A.* **100**:14920–14925.
53. Schuster, V.L. 1993. Function and regulation of collecting duct intercalated cells. *Annu. Rev. Physiol.* **55**:267–288.
54. Fejes-Toth, G., and Naray-Fejes-Toth, A. 1992. Differentiation of renal beta-intercalated cells to alpha-intercalated and principal cells in culture. *Proc. Natl. Acad. Sci. U. S. A.* **89**:5487–5491.
55. Fejes-Toth, G., and Naray-Fejes-Toth, A. 1993. Differentiation of intercalated cells in culture. *Pediatr. Nephrol.* **7**:780–784.
56. Osathanondh, V., and Potter, E.L. 1963. Development of Human kidney as shown by microdissection. III. Formation and interrelationship of collecting tubules and nephrons. *Arch. Pathol.* **76**:290–302.
57. de la Pompa, J.L., et al. 1997. Conservation of the Notch signalling pathway in mammalian neurogenesis. *Development.* **124**:1139–1148.
58. Haddon, C., Jiang, Y.J., Smithers, L., and Lewis, J. 1998. Delta-Notch signalling and the patterning of sensory cell differentiation in the zebrafish ear: evidence from the mind bomb mutant. *Development.* **125**:4637–4644.
59. Kopan, R., Nye, J.S., and Weintraub, H. 1994. The intracellular domain of mouse Notch: a constitutively activated repressor of myogenesis directed at the basic helix-loop-helix region of MyoD. *Development.* **120**:2385–2396.
60. Shawber, C., et al. 1996. Notch signaling inhibits muscle cell differentiation through a CBF1-independent pathway. *Development.* **122**:3765–3773.
61. Jones, P., et al. 1998. Stromal expression of Jagged 1 promotes colony formation by fetal hematopoietic progenitor cells. *Blood.* **92**:1505–1511.
62. Varnum-Finney, B., et al. 1998. The Notch ligand, Jagged-1, influences the development of primitive hematopoietic precursor cells. *Blood.* **91**:4084–4091.
63. Jensen, J., et al. 2000. Control of endodermal endocrine development by Hes-1. *Nat. Genet.* **24**:36–44.
64. van Es, J.H., et al. 2005. Notch/gamma-secretase inhibition turns proliferative cells in intestinal crypts and adenomas into goblet cells. *Nature.* **435**:959–963.
65. Lloyd, D.J., Hall, F.W., Tarantino, L.M., and Gekakis, N. 2005. Diabetes insipidus in mice with a mutation in aquaporin-2. *PLoS Genet.* **1**:e20.
66. McDill, B.W., et al. 2006. Congenital progressive hydronephrosis (cph) is caused by an S256L mutation in aquaporin-2 that affects its phosphoryla-

tion and apical membrane accumulation. *Proc. Natl. Acad. Sci. U. S. A.* **103**:6952–6957.
67. Rojek, A., Fuchtbauer, E.M., Kwon, T.H., Frokiaer, J., and Nielsen, S. 2006. Severe urinary concentrating defect in renal collecting duct-selective AQP2 conditional-knockout mice. *Proc. Natl. Acad. Sci. U. S. A.* **103**:6037–6042.
68. Kobayashi, T., et al. 2008. Expression and function of the Delta-1/Notch-2/Hes-1 pathway during experimental acute kidney injury. *Kidney Int.* **73**:1240–1250.
69. Terada, Y., et al. 2003. Expression and function of the developmental gene Wnt-4 during experimental acute renal failure in rats. *J. Am. Soc. Nephrol.* **14**:1223–1233.
70. Tanaka, H., et al. 2004. Expression and function of Ets-1 during experimental acute renal failure in rats. *J. Am. Soc. Nephrol.* **15**:3083–3092.
71. Behera, A.K., et al. 2004. Borrelia burgdorferi-induced expression of matrix metalloproteinases from human chondrocytes requires mitogen-activated protein kinase and Janus kinase/signal transducer and activator of transcription signaling pathways. *Infect. Immun.* **72**:2864–2871.